

Role of the cusp conditions in electron-helium double ionization

O. Chuluunbaatar and I. V. Puzynin

Joint Institute for Nuclear Research, Dubna, Moscow region 141980, Russia

P. S. Vinitsky and Yu. V. Popov

Nuclear Physics Institute, Moscow State University, Moscow 119992, Russia

K. A. Kouzakov*

*Department of Nuclear Physics and Quantum Theory of Collisions, Faculty of Physics,
Moscow State University, Moscow 119992, Russia*

C. Dal Cappello

*Université Paul Verlaine-Metz, Laboratoire de Physique Moléculaire et des Collisions, ICPMB (FR 2843),
Institut de Physique, 1 rue Arago, 57078 Metz Cedex, France*

(Received 16 January 2006; published 21 July 2006)

We develop two variational wave functions of helium which give accurate energy values and satisfy Kato's cusp conditions adapted to the variational procedure. These wave functions are utilized in calculations for reproducing the electron-helium double-ionization experimental data involving both the small and large momentum transfer. A comparison of the present numerical results for the differential cross sections with experiment indicates a minor role of the cusp conditions.

DOI: [10.1103/PhysRevA.74.014703](https://doi.org/10.1103/PhysRevA.74.014703)

PACS number(s): 34.80.Dp, 03.65.Nk, 34.10.+x

Pioneering theoretical calculations for the electron-helium double-ionization process where the scattered and two ejected electrons are detected in coincidence [1] predicted a high sensitivity of the differential cross sections to the choices of initial- and final-state wave functions of the target. The first such experiment [called $(e, 3e)$] was performed by Lahmam-Bennani *et al.* [2] at small momentum transfer. The measurements were done on an absolute scale, which provides a stringent test for the models of the initial and final states of helium. Recently, Watanabe *et al.* [3] performed electron-helium double-ionization measurements at large momentum transfer and near the Bethe ridge, where the recoil momentum of the residual ion is small compared with the transferred momentum. In this experiment [called $(e, (3-1)e)$] only the fast ejected electron is detected in coincidence with the scattered electron, while the slow ejected electron is undetected. In such kinematics the differential cross sections are primarily determined by the structure of the initial-state wave function, and hence we are lent a possibility to test various ground-state wave functions of helium. We might expect better agreement with the above experiments if more specific features of electronic correlations are taken into account in the corresponding theoretical treatments. One of such features is Kato's cusp conditions [4], which are fulfilled by the exact wave function of helium in configuration space.

Our present study is also motivated by a recent discussion [5–9] that has arisen concerning the influence of cusp conditions on the differential cross sections of $(e, 3e)$ reactions. For calculating the fivefold differential cross sections, a 3C Pluvillage model has been proposed [5]. In this model the final state of helium is treated using a 3C function [10],

which contains a product of three two-particle Coulomb waves, and the ground state is given by the Pluvillage (PL) wave function [11]

$$\Psi_{PL} = N_{PL} e^{-Z(r_1+r_2)} e^{-ikr_{12}} F_1(1 - i/2k, 2, 2ikr_{12}). \quad (1)$$

This function satisfies cusp conditions of Kato [see Eq. (4)]; however, from the spectroscopic point of view, it gives a poor value for the ground-state energy—namely, $E_{PL} = -2.8788$ a.u. (to five significant digits the exact value is -2.9037 a.u.). Nevertheless, the proposed model very well describes most of the experimental data of Lahmam-Bennani *et al.* [2], in contrast to other treatments [2,12] which are supposed to be more accurate but exhibit poor agreement with experiment. In Ref. [8] two other functions satisfying Kato's cusp conditions have been proposed. As in the PL case, in spite of giving poor energy values these two functions very well describe the experiment [2]. Let us note in this connection that the employment of the “poor” functions is mainly due to hardships associated with constructing such a variational wave function that gives an accurate energy value and satisfies the cusp conditions as well. Thus, the question arises as to whether the observed agreement with experiment owes to the fulfillment of Kato's cusp conditions, and more generally, whether the cusp conditions are important for describing the electron-helium double ionization processes or not.

Attempting to clarify the above issues, we have constructed two relatively simple wave functions that satisfy Kato's cusp conditions adapted to variational calculations (see below) and yield accurate energy values. The present method employs the variational procedure that was intensively exploited in Refs. [13,14] and demonstrated a very fast convergence. In this procedure the wave function is chosen to be of the form

*Electronic address: kouzakov@srd.sinp.msu.ru

TABLE I. The optimized values of the parameters $A_1, A_2, B_1, B_2, C_1,$ and C_2 as functions of N [see Eqs. (2) and (3)] in the case of the 2PC function.

N	A_1	A_2	B_1	B_2	C_1	C_2	$\nu_1 = \nu_2$	ν_{12}	$\mu_1 = \mu_2$	μ_{12}	E
10	1.469286	1.823331	1.539670	2.118575	0.000100	0.629076	-1.999993	0.499994	-1.931933	0.442567	-2.903630
20	1.337280	1.370111	1.209571	1.900611	0.125998	1.179287	-2.000014	0.500001	-1.935670	0.411219	-2.903705
30	1.406665	1.901167	1.291167	2.046993	0.054655	1.187195	-2.000004	0.500000	-1.959495	0.423803	-2.903720
40	0.748531	3.870564	1.057229	2.825668	0.000025	1.130515	-1.999993	0.499999	-1.953859	0.455731	-2.903721
50	1.536448	2.458788	0.601541	1.908505	0.279823	1.309478	-2.000000	0.500001	-1.951332	0.447619	-2.903723
60	0.947508	2.357829	1.038234	2.139290	0.094859	1.957289	-1.999948	0.499997	-1.955012	0.462511	-2.903724

$$\Psi(r_1, r_2, r_{12}) = \sum_{j=1}^N D_j [\exp(-\alpha_j r_1 - \beta_j r_2) + \exp(-\alpha_j r_2 - \beta_j r_1)] \exp(-\gamma_j r_{12}), \quad (2)$$

where the real parameters $\alpha_j, \beta_j,$ and γ_j are generated in a quasirandom manner:

$$\begin{aligned} \alpha_j &= \left\{ \frac{1}{2} j(j+1) \sqrt{p_\alpha} \right\} (A_2 - A_1) + A_1, \quad 0 \leq A_1 < A_2, \\ \beta_j &= \left\{ \frac{1}{2} j(j+1) \sqrt{p_\beta} \right\} (B_2 - B_1) + B_1, \quad 0 \leq B_1 < B_2, \\ \gamma_j &= \left\{ \frac{1}{2} j(j+1) \sqrt{p_\gamma} \right\} (C_2 - C_1) + C_1, \quad 0 \leq C_1 < C_2. \end{aligned} \quad (3)$$

Here $\{x\}$ designates the fractional part of x . $[A_1, A_2], [B_1, B_2],$ and $[C_1, C_2]$ are variational intervals which need to be optimized. $p_\alpha, p_\beta,$ and p_γ are some prime numbers. In this work we use the values $p_\alpha=2, p_\beta=3,$ and $p_\gamma=5$. It should be noted that the final results for $\alpha_j, \beta_j,$ and γ_j are practically insensitive to the variation of the above prime numbers.

In principle, one can supplement the variational procedure with Kato's cusp conditions [4]:

$$\begin{aligned} \frac{\partial \Psi(r_1, r_2, r_{12}) / \partial r_i |_{r_i \rightarrow 0}}{\Psi(r_1, r_2, r_{12}) |_{r_i \rightarrow 0}} &= -2 \quad (i=1,2), \\ \frac{\partial \Psi(r_1, r_2, r_{12}) / \partial r_{12} |_{r_{12} \rightarrow 0}}{\Psi(r_1, r_2, r_{12}) |_{r_{12} \rightarrow 0}} &= \frac{1}{2}. \end{aligned} \quad (4)$$

However, this is extremely difficult to realize in practice, since in that case the wave function (2) should satisfy the two-particle cusp ratios locally—i.e., in every two-particle coalescence point of configuration space. Therefore we utilize in the variational procedure the averaged two-particle cusp ratios, which follow from Eq. (4) and traditionally occur in variational calculations (see, for instance, Ref. [13]):

$$\begin{aligned} \nu_i &= [\langle \Psi | \delta(\mathbf{r}_i) (\partial / \partial r_i) | \Psi \rangle] / \langle \Psi | \delta(\mathbf{r}_i) | \Psi \rangle = -2 \quad (i=1,2), \\ \nu_{12} &= [\langle \Psi | \delta(\mathbf{r}_{12}) (\partial / \partial r_{12}) | \Psi \rangle] / \langle \Psi | \delta(\mathbf{r}_{12}) | \Psi \rangle = \frac{1}{2}. \end{aligned} \quad (5)$$

These two-particle cusp conditions can be regarded as “weak,” since they are less stringent than those given by Eq. (4). The wave function satisfying the two-particle cusp conditions given by Eq. (5) will be referred to as 2PC. One can also derive from Kato's cusp conditions (4) the cusp ratios in the three-particle coalescence point. These are given by [15,16]

$$\mu_1 = \mu_2 = \frac{\partial \Psi(r_1, r_2, r_{12}) / \partial r_1 |_{r_1, r_2, r_{12} \rightarrow 0}}{\Psi(r_1, r_2, r_{12}) |_{r_1, r_2, r_{12} \rightarrow 0}} = -2,$$

$$\mu_{12} = \frac{\partial \Psi(r_1, r_2, r_{12}) / \partial r_{12} |_{r_1, r_2, r_{12} \rightarrow 0}}{\Psi(r_1, r_2, r_{12}) |_{r_1, r_2, r_{12} \rightarrow 0}} = \frac{1}{2}. \quad (6)$$

We will refer to the wave function satisfying these three-particle cusp conditions as 3PC.

The $(e, 3e)$ experiments by Lahmam-Bennani *et al.* [2] have been examined in a first Born approximation for the interaction of the fast projectile electron with the helium atom. The final state of helium has been treated using the 3C model [10]:

$$\Psi_{3C}^-(\mathbf{p}_a, \mathbf{p}_b; \mathbf{r}_1, \mathbf{r}_2) = e^{-i\mathbf{p}_{ab} \cdot \mathbf{r}_{12}} \varphi_1^-(\mathbf{p}_a, \mathbf{r}_1) \varphi_2^-(\mathbf{p}_b, \mathbf{r}_2) \varphi_{12}^-(\mathbf{p}_{ab}, \mathbf{r}_{12}), \quad (7)$$

where \mathbf{p}_a and \mathbf{p}_b are the momenta of the ejected electrons and $\mathbf{p}_{ab} = (\mathbf{p}_a - \mathbf{p}_b)/2$; φ^- is an outgoing Coulomb wave. The fivefold differential cross section (FDCS) is given by

$$d^5\sigma/dE_a dE_b d\Omega_a d\Omega_b d\Omega_s = [2p_s p_a p_b / (2\pi)^8 p_0] |T|^2, \quad (8)$$

where p_0 and p_s are the momenta of the incident and scattered electrons, respectively. For evaluation of the amplitude T , we follow the method that was proposed in Ref. [17] for calculating the double photoionization of helium in the case of Bonham-Kohl (BK) [18] and 3C functions for the ground and final states, respectively. Using Eq. (2), the generalization of this method to the present case reads

$$\begin{aligned} T(\mathbf{Q}; \mathbf{p}_a, \mathbf{p}_b) &= -\frac{4\pi}{Q^2} \sum_{j=1}^N D_j \frac{\partial^3}{\partial \alpha_j \partial \beta_j \partial \gamma_j} \int \frac{d\mathbf{p}}{(2\pi)^3} I_{ab}(\gamma_j; \mathbf{p}_{ab}, \mathbf{p} \\ &+ \mathbf{p}_{ab}) [I_a(\alpha_j; \mathbf{p}_a, \mathbf{Q} - \mathbf{p}) I_b(\beta_j; \mathbf{p}_b, \mathbf{p}) + I_a(\alpha_j; \mathbf{p}_a, \\ &- \mathbf{p}) I_b(\beta_j; \mathbf{p}_b, \mathbf{Q} + \mathbf{p}) - 2I_a(\alpha_j; \mathbf{p}_a, \\ &- \mathbf{p}) I_b(\beta_j; \mathbf{p}_b, \mathbf{p})], \end{aligned} \quad (9)$$

where $\mathbf{Q} = \mathbf{p}_0 - \mathbf{p}_s$ is the momentum transfer and

$$\begin{aligned} I_\tau(\lambda; \mathbf{p}_\tau, \mathbf{k}) &= \int \frac{d\mathbf{r}}{r} \varphi^{*-}(\mathbf{p}_\tau, \mathbf{r}) e^{-\lambda \mathbf{r} + i\mathbf{k} \cdot \mathbf{r}} = 4\pi R(\xi_\tau) \\ &\times \frac{[(\lambda - ip_\tau)^2 + k^2]^{i\xi_\tau}}{[(\mathbf{k} - \mathbf{p}_\tau)^2 + \lambda^2]^{1+i\xi_\tau}} \quad (\tau = a, b, ab). \end{aligned} \quad (10)$$

Here $\xi_a = -2/p_a, \xi_b = -2/p_b,$ and $\xi_{ab} = 1/p_{ab}$ are the Coulomb numbers and $R(\xi) = e^{-\pi\xi/2} \Gamma(1+i\xi)$.

Table I presents the values of the parameters $A_1, A_2, B_1, B_2, C_1,$ and C_2 optimized in the case of two-particle cusp conditions (5) for different values of N in Eq. (2). Here E is a minimized energy value (in a.u.) for the ground state of helium. The calculated values of $\nu_1 = \nu_2, \nu_{12}, \mu_1 = \mu_2,$ and μ_{12}

TABLE II. The same as in Table I, but in the case of the 3PC function.

N	A_1	A_2	B_1	B_2	C_1	C_2	$\mu_1=\mu_2$	μ_{12}	$\nu_1=\nu_2$	ν_{12}	E
10	0.766311	2.208667	1.855175	2.006284	0.000000	1.353692	-1.999966	0.499980	-2.009074	0.504688	-2.903316
20	0.419230	4.534614	1.215131	1.701001	0.000000	1.861596	-2.000003	0.499993	-1.980331	0.739926	-2.903650
30	0.255876	4.688463	1.173995	1.759000	0.000000	1.773162	-2.000017	0.500005	-2.016875	0.516822	-2.903691
40	0.547070	3.139303	0.358449	3.247590	0.122527	1.770810	-1.999998	0.500001	-2.018721	0.374982	-2.903696
50	0.586607	3.120426	0.644193	3.237636	0.248869	1.770040	-1.999990	0.499992	-2.018229	0.534080	-2.903708
60	0.337056	4.575246	0.243134	2.620192	0.058266	2.388388	-2.000000	0.500000	-2.005584	0.481663	-2.903721

indicate the quality of the cusp ratios. Table II presents the analogous results in the case of three-body cusp conditions (6). As can be seen, in both cases the calculated cusp ratios for $N=60$ are in good agreement with exact ones, $\nu_1=\nu_2=\mu_1=\mu_2=-2$ and $\nu_{12}=\mu_{12}=0.5$, and yield the energy values $E=-2.903\,724$ a.u. and $E=-2.903\,721$ a.u., respectively (to seven significant digits the exact value is $-2.903\,724$ a.u.). Table III displays the coefficients D_j of the sum on the right-hand side of Eq. (2) when $N=60$.

Figure 1 shows the numerical results for the $(e,3e)$ measurements performed by Lahmam-Bennani *et al.* [2]. In this setup all three outgoing electrons are detected in the same plane. The incident electron energy is $E_0=5599$ eV. The scattered electron energy and angle are $E_s=5500$ eV and $\theta_s=0.45^\circ$, respectively. The ejected electron energies are $E_a=E_b=10$ eV. As can be seen, the 2PC and 3PC functions give almost identical results, which are visually indistinguishable and are very close to those using a BK function [8]. Also are shown the results using the helium function by Le Sech [15]. Such a choice is motivated by the fact that the BK function gives a rather accurate energy value ($E_{BK}=-2.9035$ a.u.) but does not satisfy the cusp conditions even in the three-particle coalescence point, while the Le Sech function exactly satisfies the cusp conditions in the

three-particle coalescence point but gives a less accurate energy value ($E_{LS}=-2.9020$ a.u.). Note that in the cases $\theta_a=83^\circ$ and $\theta_a=207^\circ$ the results using the PL function, which are presented in Refs. [5,8], exhibit similar disagreement with the experiment.

Figure 2 shows the numerical results for the recent symmetric noncoplanar $(e,(3-1)e)$ and $(e,2e)$ experiments by Watanabe *et al.* [3]. In these experiments two fast outgoing electrons, the scattered and ejected ones, having equal energies ($E_s=E_a=1000$ eV) and polar angles ($\theta_s=\theta_a=45^\circ$) are detected. In the $(e,(3-1)e)$ case, the slow ejected electron, which is not detected, has energy $E_b=10$ eV. The $(e,2e)$ and $(e,(3-1)e)$ cross sections are studied as functions of the momentum $q=|\mathbf{p}_s+\mathbf{p}_a-\mathbf{p}_0|$. The calculations have been performed in the plane-wave impulse approximation (PWIA), and these results have been folded with the experimental momentum resolution (see Ref. [3] for details). In the $(e,(3-1)e)$ case the results using the 2PC and 3PC are very close to each other and also to those using the BK function. Interestingly, the PL function better reproduces the $(e,(3-1)e)$ experiment on an absolute scale, but it clearly fails in the case of $(e,2e)$ transition to the $n=2$ excited state of He^+ . The marked discrepancies between theory and experiment in Fig. 2 show that the PWIA model is insufficient for a de-

TABLE III. The expansion coefficients D_j of the 2PC and 3PC functions for $N=60$ [see Eq. (2)].

j	2PC	3PC	j	2PC	3PC	j	2PC	3PC
1	95.677982873592	-15.555950678025	21	4.132349862703	0.976229699411	41	-232.551883020903	-0.020801940364
2	63.849737004101	4.370218508660	22	-6.685238500807	-11.419625081681	42	-0.027886569611	-0.000034504456
3	48.779553550446	-15.523087015389	23	0.098154786811	-0.008827390881	43	-196.796001785021	-52.414228081091
4	15.010459053761	-0.038468454213	24	226.107857120258	-10.831947483531	34	145.841243468623	-8.934151126271
5	194.285160635442	-73.542233585401	25	-472.063482737854	-2.601375880982	45	757.452970529460	150.152702267692
6	268.555839725773	-49.460818952469	26	111.862825443534	24.240916733832	46	-32.125103104848	1.396415741634
7	-311.991934522318	-43.547416698060	27	-302.505859300812	-50.505963942900	47	162.194224573393	3.482227887395
8	143.224101742417	49.606837796527	28	-11.080466438934	2.252948726397	48	-215.149006425032	8.779400169379
9	341.371403246133	6.283910345646	29	-92.571338910105	-5.804774151965	49	142.144431461679	26.445362209468
10	-56.775690460802	30.223649108785	30	-178.603509400750	7.025498959928	50	13.645733152307	-0.865624203969
11	-7.619623443503	8.632956153639	31	0.287768263079	-0.005244592666	51	2.569190588268	2.635131521561
12	-21.978830636145	-0.046365077329	32	1489.177015048587	118.491148431040	52	119.250555855200	-22.259398311014
13	-736.626687704224	-142.166666838168	33	-176.621853409999	-87.025650728786	53	4380.793861101516	-29.643755008429
14	-4473.013177518544	-17.923251212093	34	182.581206746621	174.365321843475	54	0.792261961533	0.020296371325
15	-312.136887809310	-2.479221895137	35	2.408741991808	-6.728759386956	55	-230.135481686892	-32.211777489026
16	-7.201184787943	-4.285596670384	36	35.490640614116	9.313371385535	56	-25.563328110971	-2.533987792133
17	-0.088161313620	0.005573357410	37	-69.351368477907	0.388197705828	57	-11.444497132713	0.047170696616
18	-4.077442893985	-2.109938254985	38	1.894014772691	-4.845301156286	58	-694.744658815902	21.876663239848
19	112.285131475145	-1.856650794380	39	1.466875923440	-0.065850546125	59	-205.457909795614	14.748945832116
20	5.018614980845	4.352262068407	40	17.452064490678	27.833783986858	60	-0.031448873308	-0.000243625440

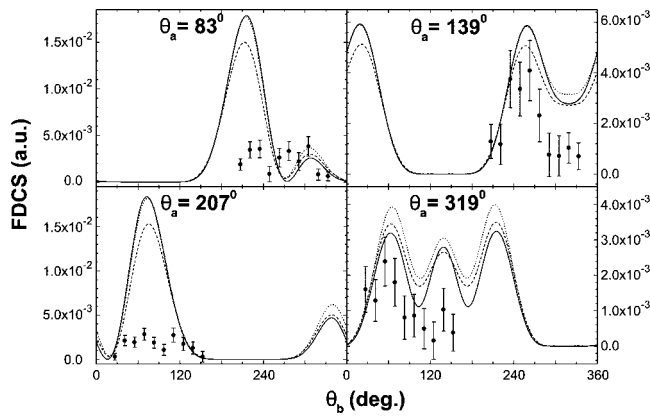


FIG. 1. FDCS for the $(e,3e)$ experiment [2]. Theoretical curves are the results of the 3C calculations using the following wave functions of helium: 2PC (solid line), BK (dashed line), and Le Sech (dotted line).

scription of ionization-excitation and double ionization in the considered kinematical regime. One encounters a similar situation in the case of ionization-excitation of a hydrogen molecule [19]. These observations call for new experiments at higher incident energies in order to test the validity of the PWIA.

In summary, we have constructed and tabulated variational wave functions for the ground state of helium, which satisfy the cusp conditions (5) and (6) and provide accurate energy values. We have utilized these functions in calculating the electron-impact double-ionization cross sections on helium [2,3] and compared these cross sections with the corresponding measured data. From the results of the present study we can conclude that in the considered experiments the cusp conditions do not play any appreciable role and the observed discrepancies between theory and experiment can be attributed to deficiencies of the approximations used for the final state (see also Refs. [3,6]). In addition, the initial-state functions giving accurate energy values for the ground state of helium exhibit similar results for cross sections in the framework of the 3C and PWIA models, irrespective of whether these functions satisfy the cusp conditions or not. This observation reflects the fact that for determining the cross sections the “averaged” behavior of the initial-state function in configuration space is much more crucial than its

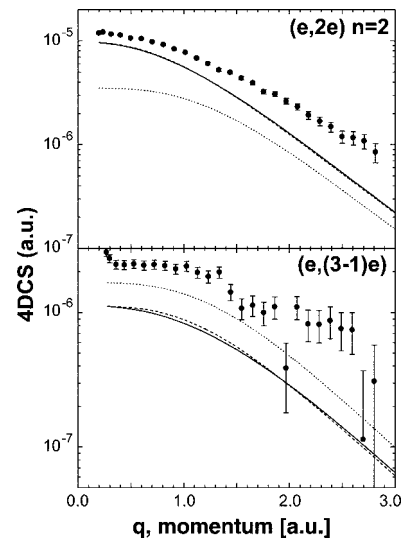


FIG. 2. The triple (upper panel) and fourfold (lower panel) differential cross sections, TDCS and 4DCS, for the $(e,2e)$ and $(e,(3-1)e)$ experiments [3], respectively. The curves are the results of PWIA calculations, convoluted with the experimental resolution function, using the following wave functions of helium: 2PC (solid line), BK (dashed line), and PL (dotted line).

behavior in the small regions of configuration space where Kato’s cusp conditions dominate.

One might expect the effect of the cusp conditions to be negligible in the kinematics that involves small energy and momentum transfer, since the multiple-rescattering effects due to an escape of a slow electron pair from helium strongly overshadow information on the initial-state correlations. In this regard, the kinematics near the Bethe ridge (for example, see Fig. 2) seems more sensible to the cusp conditions if the incident electron energy is high enough for neglecting the higher-order Born contributions. In such kinematics large values of the momentum q correspond to small values of the electron coordinate r and hence allow one to probe the domain where the cusp condition dominates.

We are very grateful to Azzedine Lahmam-Bennani for communicating his experimental results and to Noboru Watanabe for providing us with the computer code which convolutes theoretical calculations with the experimental resolution function. We are also indebted to Amulya Roy for valuable comments and suggestions.

[1] B. Joulakian and C. Dal Cappello, *Phys. Rev. A* **47**, 3788 (1993).
 [2] A. Lahmam-Bennani *et al.*, *Phys. Rev. A* **59**, 3548 (1999).
 [3] N. Watanabe *et al.*, *Phys. Rev. A* **72**, 032705 (2005).
 [4] T. Kato, *Commun. Pure Appl. Math.* **10**, 151 (1957).
 [5] S. Jones and D. H. Madison, *Phys. Rev. Lett.* **91**, 073201 (2003).
 [6] J. Berakdar, *Phys. Rev. Lett.* **92**, 149301 (2004); S. Jones and D. H. Madison, *ibid.* **92**, 149302 (2004).
 [7] S. Jones *et al.*, *Phys. Rev. A* **70**, 012712 (2004).
 [8] L. U. Ancarani *et al.*, *Phys. Rev. A* **70**, 012711 (2004).
 [9] S. Jones *et al.*, *Phys. Rev. A* **72**, 012718 (2005).
 [10] M. Brauner *et al.*, *J. Phys. B* **22**, 2265 (1989).

[11] P. Pluvinaige, *Ann. Phys. (Paris)* **5**, 145 (1950); *J. Phys. Radium* **12**, 789 (1951).
 [12] A. Kheifets *et al.*, *J. Phys. B* **32**, 5047 (1999).
 [13] A. M. Frolov, *Phys. Rev. A* **57**, 2436 (1998).
 [14] V. I. Korobov, *Phys. Rev. A* **61**, 064503 (2000).
 [15] C. Le Sech, *J. Phys. B* **30**, L47 (1997).
 [16] Yu. V. Popov and L. U. Ancarani, *Phys. Rev. A* **62**, 042702 (2000).
 [17] M. A. Kornberg and J. E. Miraglia, *Phys. Rev. A* **48**, 3714 (1993).
 [18] R. A. Bonham and D. A. Kohl, *J. Chem. Phys.* **45**, 2471 (1966).
 [19] M. Takahashi *et al.*, *Phys. Rev. A* **68**, 042710 (2003).